Analysis of Time-Distributed Model Predictive Control when using a Regularized Primal-Dual Gradient Optimizer

Terrence Skibik, Marco M. Nicotra

***Abstract*— Time-distributed Optimization (TDO) is a method for reducing the computational cost of Model Predictive Control (MPC) where optimization iterations are distributed over time by maintaining a running solution estimate that is updated at each sampling instant. In this paper, TDO is applied to linear MPC with state and input constraints using a regularized primal-dual gradient descent method as the optimizer. A detailed analysis of the rate of convergence shows how different design choices, i.e. maximum number of iterations, value of the regularization term, and prediction horizon length, affect the stability of TDO-MPC. Additionally, it is shown that significant stability improvements can be achieved by using the Closed-Loop Paradigm to improve the conditioning number of the optimal control problem. Numerical simulations on an open-loop unstable system demonstrate the overall impact on stability and constraint satisfaction of each design choice.**

***Index Terms*— Optimization, Optimal control, Stability analysis, Real-time systems, Predictive control**

I. Introduction

MODEL Predictive Control (MPC) is a feedback policy that enacts the solution to a receding horizon Optimal Control Problem (OCP) at every sampling instant [1]. Despite the overall success of MPC, the main bottleneck for its widespread adoption is the fact that, depending on the system complexity, hardware specifications, and sampling rate, solving the OCP in real-time may not be feasible.

An approach to help reduce the computational complexity of the OCP is to distribute the optimizer iterations over multiple time steps while ensuring important properties of the closed-loop system (e.g. asymptotic stability, recursive feasibility) are retained. This method, known as Time-distributed Optimization (TDO) [2], relies on a running solution estimate that is refined at each time step by performing a fixed number of solver iterations. The suboptimal control input is then given to the system which evolves according to its dynamics, thereby creating a feedback loop between the plant and optimizer, as shown in Figure 1.

Various properties of suboptimal MPC have been studied in literature including performance, stability, and robustness. Control schemes using continuous-time optimizer dynamics are in investigated in [3]–[5]. Suboptimal MPC of unconstrained discrete-time nonlinear systems is studied in [6] and their stability is investigated in [7] in the absence of constraints. A detailed stability analysis of linear systems subject to input constraints can be found in [8], [9].

T. Skibik and M. M. Nicotra are with the University of Colorado, Boulder, Email: {terrence.skibik, marco.nicotra}@colorado.edu.

This research is supported by the National Science Foundation Award Number CMMI 1904441.

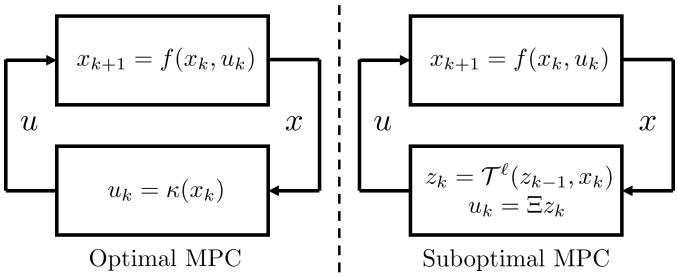

Fig. 1. Suboptimal MPC can be interpreted as a feedback interconnection between the plant and an optimization algorithm with a solution estimate z as its internal state, k the time index, dynamics defined by ℓ iterations of the algorithm $\mathcal{T}^\ell$, and a output selection matrix Ξ.

This paper extends the results from [9], which is limited to input constraints, by handling both state and input constraints, which are addressed using a regularized primal-dual algorithm since it allows for a significant amount of transparency in the stability analysis. Using Input-to-State Stability (ISS) techniques, we derive an analytic expression for the optimizer gain, show a sufficient condition for asymptotic stability using the small gain theorem, and explore how the various system parameters affect these properties. Moreover, we show how the use of the Closed-Loop Paradigm for MPC [10] can significantly improve the stability of the interconnected closed-loop system at no additional cost.

A. Notation

The normal cone mapping of a convex set $\mathcal{C}$ is defined as

$$\mathcal{N}_{\mathcal{C}}(v) = \begin{cases} \{y \mid y^T(w-v) \leq 0, \forall w \in \mathcal{C}\}, & \text{if } v \in \mathcal{C}, \\ \emptyset & \text{else.} \end{cases}$$

For matrices $A \in \mathbb{R}^{n\times m}$ and $B \in \mathbb{R}^{p\times q}$; $A \otimes B \in \mathbb{R}^{np\times mq}$ denotes the Kronecker product. Let $\mathbb{R}^n_+ \subset \mathbb{R}^n$ be the positive orthant and $(\mathbb{S}^n_{++}, \mathbb{S}^n_+)$ denote the set of symmetric $n \times n$ positive (definite, semidefinite) matrices. Given $x \in \mathbb{R}^n$ and $W \in \mathbb{S}^n_{++}$, the W-norm of x is $\|x\|_W = \sqrt{x^T W x}$ and the maximum and minimum eigenvalues of W are denoted $\lambda^+(W)$ and $\lambda^-(W)$. For two vectors $x \in \mathbb{R}^n$, $y \in \mathbb{R}^m$, the

vector $(x, y) = [x^T \ y^T]^T \in \mathbb{R}^{n+m}$. We use $I_n \in \mathbb{R}^{n\times n}$ and $0_{n\times m} \in \mathbb{R}^{n\times m}$ to denote the identify and zero matrix. The subscripts are omitted when the dimensions are apparent. A vector of N 1's is denoted 1_N, the standard basis vectors are $\mathbb{1}_i$, and the projection onto a convex set $\mathcal{C}$ is $\Pi_{\mathcal{C}}(\cdot)$.

II. Problem Setting

Consider a Linear Time Invariant (LTI) system

$$x_{k+1} = Ax_k + Bu_k, \tag{1}$$

where $x \in \mathbb{R}^n$ is the state and $u \in \mathbb{R}^m$ is the control input. The control objective is stabilize the origin of (1) while enforcing pointwise-in-time constraints

$$x_k \in \mathcal{X}, \ u_k \in \mathcal{U}, \ \forall k \in \mathbb{N} \tag{2}$$

Assumption 1. *The constraint set $\mathcal{X} \times \mathcal{U}$ is a closed, convex polyhedra, and contains the origin in its interior.*

A natural way to approach this constrained problem is with MPC. Consider the following Parameterized Optimal Control Problem (POCP) with parameter x

$$\begin{aligned}
\min_{\mu} \quad & \frac{1}{2}\|\xi_N\|_P^2 + \frac{1}{2}\sum_{i=0}^{N-1} \|\xi_i\|_Q^2 + \|\mu_i\|_R^2, && && \text{(3a)}\\
\text{s.t.} \quad & \xi_{i+1} = A\xi_i + B\mu_i, && i = 0, \dots, N-1, && \text{(3b)}\\
& \xi_i \in \mathcal{X}, \ \mu_i \in \mathcal{U}, && i = 0, \dots, N-1, && \text{(3c)}\\
& \xi_0 = x, \ \xi_N \in \mathcal{X}_N && && \text{(3d)}
\end{aligned}$$

where $N > 0$ the horizon length, $Q \in \mathbb{R}^{n\times n}, R \in \mathbb{R}^{m\times m}$ and $P \in \mathbb{R}^{n\times n}$ are weighting matrices, $x \in \mathbb{R}^n$ is the current system state, $\mu = (\mu_0, \dots, \mu_{N-1})$, $\xi = (\xi_0, \dots, \xi_N)$, and $\mathcal{X}_N \subset \mathbb{R}^n$ is a polyhedral terminal set.

The MPC feedback law can then be defined as $u = \Xi\mu^*(x)$, where $\Xi = \mathbb{1}_1 \otimes I_m$ selects μ_0 from μ and $\mu^*(x)$ is the solution to (3) for the parameter value x. To ensure that (3) can be used to construct a stabilizing feedback law for (1), we make the following assumptions.

Assumption 2. *The pair (A, B) is stabilizable and the cost matrices satisfy $R \in \mathbb{S}_{++}^m$, $Q \in \mathbb{S}_{+}^n$, and (A, Q) observable.*

Assumption 3. *The terminal set $\mathcal{X}_N$ contains the origin in its interior, is constraint admissible, and is positively invariant under the fictitious terminal control law $u_N(x) = -Kx$. Given $x \in \mathcal{X}_N$ and a gain K, the terminal cost satisfies $P = Q + A^TPA - (A^TPB)(R + B^TPB)^{-1}(B^TPA) \in \mathbb{S}_{++}^n$.*

A typical way to solve (3) is using an iterative optimization algorithm. In this paper, we address the case that there are not enough computational resources available to solve (3) to completion at every sampling instant. Instead, we utilize TDO by performing a finite number of iterations $\ell \in (0, \infty)$ and warmstarting the optimization algorithm using the suboptimal solution from the previous sampling instant. The plant-optimizer dynamics are then

$$\begin{aligned}
z_k &= \mathcal{T}^\ell(z_{k-1}, x_k), && \text{(4a)}\\
x_{k+1} &= Ax_k + B\Xi z_k, && \text{(4b)}
\end{aligned}$$

where z_k denotes the running solution estimate (i.e. the suboptimal solution) at time instant k and $\mathcal{T}^\ell$ is the output of the optimization algorithm after ℓ steps.

III. Optimization Strategy

To efficiently handle the constraints, we first note that the equality constraints of (3) can be written in the form

$$\xi = \hat{A}x + \hat{B}\mu, \tag{5}$$

where

$$\hat{B} = \begin{bmatrix} 0 & \cdots & 0 \\ B & \ddots & \vdots \\ \vdots & \ddots & 0 \\ A^{N-1}B & \cdots & B \end{bmatrix}, \text{ and } \hat{A} = \begin{bmatrix} I \\ A \\ \vdots \\ A^N \end{bmatrix}. \tag{6}$$

Additionally, since the constraint sets are polyhedral by Assumption 1, we may rewrite (3c) in the form

$$C\xi_i + D\mu_i \le h, \text{ for } i = 0 \ , \dots \ , N-1. \tag{7}$$

where $C \in \mathbb{R}^{p\times n}$, $D \in \mathbb{R}^{p\times m}$, and $h \in \mathbb{R}^p$. Substituting (5) into (3a), and replacing (3c) with (5) substituted into (7) we arrive at the standard condensed form [1]

$$\begin{aligned}
\min_{\mu\in\bar{\mathcal{U}}} \quad & f(\mu, x) = \frac{1}{2}\mu^T H\mu + \mu^T Gx + \frac{1}{2}x^T Wx, && \text{(8a)}\\
\text{s.t.} \quad & E\mu + Fx \le d. && \text{(8b)}
\end{aligned}$$

where $\bar{\mathcal{U}} = \mathcal{U}^N$ and the cost matrices are $\hat{R} = I_N \otimes R$, $H = \hat{B}^T\hat{H}\hat{B} + \hat{R}$, $G = \hat{B}^T\hat{H}\hat{A}$, $W = Q + \hat{A}^T\hat{H}\hat{A}$, $\hat{C} = \begin{bmatrix} I_N \otimes (C - DK) & 0_{p\times n} \end{bmatrix}$, $\hat{D} = I_N \otimes D$, $E = \hat{C}\hat{B} + \hat{D}$, $F = \hat{C}\hat{A}$, $d = (1_N \otimes h)$, and $\hat{H} = \begin{bmatrix} (I_N \otimes Q) & 0 \\ 0 & P \end{bmatrix}$. As detailed in [1], it follows from Assumption 2 that $H \in \mathbb{S}_{++}$.

A. Optimization Algorithm

To solve the Quadratic Program (QP) (8), we employ a regularized primal-dual algorithm [11]. The regularized Lagrangian for the problem is

$$\mathcal{L}_\epsilon(\mu, \lambda, x) = \frac{1}{2}\mu^T H\mu + \mu^T Gx + \lambda^T(E\mu + Fx - d) - \frac{\epsilon}{2}\|\lambda\|_2^2, \tag{9}$$

where $\lambda \in \mathbb{R}^q$ is the dual variable associated with the inequality constraints, and $\epsilon > 0$ is the regularization parameter. An important property of (9) is that it is strongly convex in μ and strongly concave in λ. These properties allow us to derive a convergence result which is sufficient to prove ISS stability of the algorithm. Additionally, the following pair of Variational Inequalities (VI) are both necessary and sufficient for optimality [12],

$$\begin{aligned}
-\nabla_\mu \mathcal{L}_\epsilon(\mu, \lambda, x) &\in \mathcal{N}_{\bar{\mathcal{U}}}(\mu), && \text{(10a)}\\
\nabla_\lambda \mathcal{L}_\epsilon(\mu, \lambda, x) &\in \mathcal{N}_{\mathbb{R}_+^p}(\lambda). && \text{(10b)}
\end{aligned}$$

Remark 1. *The VI (10b) is sufficient for optimality since it enforces the gradient, positivity, and complementary slackness conditions for the dual variables. Additionally, we know the duality gap is zero, and we require no constraint qualifiers*

since the cost function is quadratic and the inequality constraints are affine.

The solution mapping of the algorithm can be written as

$$S(x) = \mathcal{A}^{-1}(-\bar{G}x - \bar{d}), \quad \mathcal{A} = \bar{H} + \mathcal{N}_{\mathcal{Z}} \tag{11}$$

with $\mathcal{Z} = \bar{\mathcal{U}} \times \mathbb{R}^q_+$, $\bar{H} = \begin{bmatrix} H & E^T \\ -E & \epsilon I \end{bmatrix}$, $\bar{G} = \begin{bmatrix} G \\ -F \end{bmatrix}$, and $\bar{d} = \begin{bmatrix} 0 \\ d \end{bmatrix}$. Primal-dual algorithms work by descending in the primal variable and ascending in the dual variable to find the saddle-point of the Lagrangian. Letting $z = (\mu, \lambda)$, a single primal-dual step can be concisely written as

$$z^{j+1} = \Pi_{\mathcal{Z}}(z^j - \alpha\Phi(z^j)) \tag{12}$$

where α is the step size and the mapping Φ is defined as

$$\Phi(z) = \begin{bmatrix} \nabla_\mu \mathcal{L}_\epsilon(z,x) \\ -\nabla_\lambda \mathcal{L}_\epsilon(z,x) \end{bmatrix} = \begin{bmatrix} H\mu + Gx + E^T\lambda \\ -E\mu - Fx + d + \epsilon\lambda \end{bmatrix}. \tag{13}$$

The following Lemma explicitly computes the strong monotonicity and Lipschitz continuity constants of the mapping Φ as a function of H, E, and ϵ.

Lemma 1. *Let Assumptions 1–3 hold and let $\epsilon > 0$. Then, the regularized mapping Φ is strongly monotone and Lipschitz over $\mathcal{Z}$ with constant $\eta_\Phi(\epsilon) = min\{\lambda^-(H), \epsilon\}$ and $L_\Phi(\epsilon) = \sqrt{\lambda^+(\Gamma)}$, where*

$$\Gamma = \begin{bmatrix} H^2 + E^TE & (H - \epsilon I)E^T \\ E(H - \epsilon I) & \epsilon^2 I + EE^T \end{bmatrix}.$$

Proof: First we show Φ is strongly monotone. For two vectors $z_1 = (\mu_1, \lambda_1)$, $z_2 = (\mu_2, \lambda_2) \in \bar{\mathcal{U}} \times \mathbb{R}^q_+$, we have

$$\begin{aligned}
&(\Phi(z_1) - \Phi(z_2))^T(z_1 - z_2) \\
&= \|\mu_1 - \mu_2\|_H^2 + \langle(\mu_1 - \mu_2), E^T(\lambda_1 - \lambda_2)\rangle \\
&- \langle(\lambda_1 - \lambda_2, E(\mu_1 - \mu_2)\rangle + \epsilon\|\lambda_1 - \lambda_2\|_2^2 \\
&= \|\mu_1 - \mu_2\|_H^2 + \epsilon\|\lambda_1 - \lambda_2\|_2^2 \\
&= (z_1 - z_2)^T\tilde{H}(z_1 - z_2) \\
&\geq \min\{\lambda^-(H), \epsilon\}\|z_1 - z_2\|_2^2,
\end{aligned}$$

where $\tilde{H} = \begin{bmatrix} H & 0 \\ 0 & \epsilon I \end{bmatrix}$. Thus, $(\Phi(z_1) - \Phi(z_2))^T(z_1 - z_2) \geq \min\{\lambda^-(H), \epsilon\}\|z_1 - z_2\|_2^2$ which gives us our strong monotonicity constant $\eta_\Phi(\epsilon) = \min\{\lambda^-(H), \epsilon\}$ since $H \in \mathbb{S}_{++}$.

Next, we show that Φ is Lipschitz on its domain. For two vectors $z_1 = (\mu_1, \lambda_1)$, $z_2 = (\mu_2, \lambda_2) \in \bar{\mathcal{U}} \times \mathbb{R}^q_+$, we have

$$\begin{aligned}
&\|\Phi(z_1) - \Phi(z_2)\|_2^2 \\
&= (\mu_1 - \mu_2)^T HH(\mu_1 - \mu_2) + 2(\mu_1 - \mu_2)^T HE^T(\lambda_1 - \lambda_2) \\
&+ (\lambda_1 - \lambda_2)^T EE^T(\lambda_1 - \lambda_2) + (\mu_1 - \mu_2)^T E^T E(\mu_1 - \mu_2) \\
&- 2\epsilon(\mu_1 - \mu_2)^T E^T(\lambda_1 - \lambda_2) + \epsilon^2(\lambda_1 - \lambda_2)^T(\lambda_1 - \lambda_2) \\
&= (z_1 - z_2)^T \begin{bmatrix} H^2 + E^TE & (H - \epsilon I)E^T \\ E(H - \epsilon I) & \epsilon^2 I + EE^T \end{bmatrix}(z_1 - z_2).
\end{aligned}$$

This gives us the relation

$$\|\Phi(z_1) - \Phi(z_2)\|_2^2 \leq \lambda^+(\Gamma)\|z_1 - z_2\|_2^2,$$

leading to the Lipschitz constant $L_\Phi(\epsilon) = \sqrt{\lambda^+(\Gamma)}$.

A single iteration of (12) is represented by

$$z^{j+1} = \mathcal{T}(z^j, x), \tag{14}$$

where $\mathcal{T} : \mathbb{R}^{Nm} \times \mathbb{R}^q \times \mathbb{R}^n \to \mathbb{R}^{Nm} \times \mathbb{R}^q$. When running the algorithm for multiple iterations, we have the following recursive definition for $\mathcal{T}^\ell$

$$\mathcal{T}^\ell(z, x) = \mathcal{T}(\mathcal{T}^{\ell-1}(z, x), x), \tag{15}$$

where $z \in \mathbb{R}^{Nm} \times \mathbb{R}^q$ is the solution estimate, x the input parameter, and $\mathcal{T}^0(z, x) = z$. The following theorem explicitly defines the convergence properties of the regularized primal-dual gradient algorithm as a function of H, E, and ϵ.

Theorem 1. *Suppose Assumptions 1–3 hold. Let $\mathcal{T}^\ell$ represent ℓ steps of the regularized primal-dual (12), and pick any $x \in \mathbb{R}^n$. Then, for any $z \in \mathbb{R}^{Nm} \times \mathbb{R}^q$,*

$$\|\mathcal{T}^\ell(z, x) - S(x)\|_2 \leq \rho^\ell\|z - S(x)\|_2,$$

where $\rho = max\{|1 - \alpha\eta_\Phi|, |1 - \alpha L_\Phi|\}$ and $\alpha \in (0, 2/L_\Phi)$.

Proof: Using the standard approach to proving convergence for strongly convex, smooth cost functions, we have

$$\begin{aligned}
&\|\mathcal{T}^\ell(z, x) - S(x)\|_2, \\
&= \|\Pi_{\mathcal{Z}}[\mathcal{T}^{\ell-1}(z, x) - \alpha\Phi(\mathcal{T}^{\ell-1}(z, x))] - S(x)\|_2, \\
&= \|\Pi_{\mathcal{Z}}[\mathcal{T}^{\ell-1}(z, x) - \alpha\Phi(\mathcal{T}^{\ell-1}(z, x))] \\
&\qquad - \Pi_{\mathcal{Z}}[S(x) - \alpha\Phi(S(x))]\|_2, \\
&\leq \|(\mathcal{T}^{\ell-1}(z, x) - S(x)) - \alpha(\Phi(\mathcal{T}^{\ell-1}(z, x)) - \Phi(S(x)))\|_2.
\end{aligned}$$

Where the last step is from the non-expansivity of the projection operator. From Lemma 1, we know Φ is strongly monotone and Lipschitz so $\|I - \alpha\Phi\| \leq \max\{|1 - \alpha\eta_\Phi|, |1 - \alpha L_\Phi|\}$. If we let $\rho = \max\{|1 - \alpha\eta_\Phi|, |1 - \alpha L_\Phi|\}$, we have

$$\begin{aligned}
\|\mathcal{T}^\ell(z, x) - S(x)\|_2 &\leq \rho\|\mathcal{T}^{\ell-1}(z, x) - S(x)\|_2 \\
&\leq \rho^\ell\|\mathcal{T}^0(z, x) - S(x)\|_2
\end{aligned}$$

Then, for $\alpha \in \left(0, \frac{2}{L_\Phi}\right)$ we have $\rho < 1$.

Remark 2. *The regularization term $\epsilon > 0$ is essential for our analysis of the primal-dual algorithm. Although $S(x)$ is not the true solution to the QP (8), [13] has a bound on the suboptimality of the solution. If we define $(\bar{\mu}^*, \bar{\lambda}^*) = S(x)$ we have the bound*

$$\|\mu^* - \bar{\mu}^*\| + \frac{\epsilon}{2}\|\bar{\lambda}^*\| \leq \frac{\epsilon}{2}\|\lambda^*\|, \ \forall\lambda^* \in \mathcal{D}^*,$$

where $\mathcal{D}^* \subset \mathbb{R}^q_+$ is a bounded subset of $\mathbb{R}^q_+$ used to ensure $\|\lambda\|$ is bounded. Since the goal of our MPC is to drive the state of the system to the origin, which is strictly inside the constraint set by Assumption 1, all the inequality constraints will eventually become inactive. As a result, we can take $\mathcal{D}^* = \{0\}$ to recover

$$\|\mu^* - \bar{\mu}^*\| = 0.$$

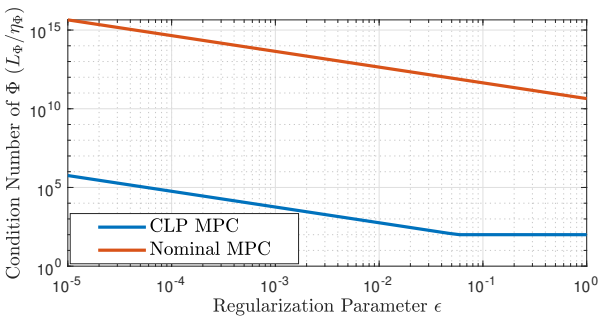

Fig. 2. The effect of the CLP-MPC on the condition number of Φ for the inverted pendulum example in Section V.

B. Closed-Loop Paradigm

Although the convergence proof in Theorem 1 gives us a range of allowable step sizes for (12), we will use $\alpha = 2/(L_\Phi + \eta_\Phi)$ for the remainder of the paper. This choice of α maximizes the worst case convergence rate [14] of the algorithm (12). This choice leads to $\rho = (\kappa-1)/(\kappa+1)$ where $\kappa = L_\Phi(\epsilon)/\eta_\Phi(\epsilon)$ is the conditioning number of Φ.

Since the convergence rate of our primal-dual algorithm is strongly tied to the conditioning of Φ, we make use of the Closed-Loop Paradigm (CLP) [10] to improve the conditioning of our problem. The CLP effectively pre-staiblizes the system by introducing a feedback gain K and redefining the control inputs as $u_k = -Kx_k + w_k$, $\forall k \in (0, N-1)$ where w_k becomes our new optimization variable. Choosing $K = (R + B^TPB)^{-1}B^TPA$ (i.e. the optimal LQR gain), our new QP becomes

$$\min_{\omega} \quad f(\omega, x) = \frac{1}{2}\omega^T(I_N \otimes (B^TPB + R))\omega + \frac{1}{2}x^TPx, \tag{16a}$$

$$\text{s.t.} \quad E\omega + Fx \leq d, \tag{16b}$$

where any use of A is replaced by $(A-BK)$ in (6) and C by $(C - DK)$ in (7). Note that the CLP QP has a unique form where $H = I_N \otimes (B^TPB+R)$, and $G = 0$ which significantly improves the conditioning of H as seen in Figure 2.

IV. Stability Analysis of the Coupled System

In this section, we analyze the closed loop dynamics of the coupled system (4) using the ISS framework. The analysis of the nominal MPC and the Closed-Loop Paradigm is identical except for the variable changes discussed after (16). This analysis extends the general guidelines established in [9] to the regularized primal-dual gradient descent.

A. Solution Mapping Properties

We begin by deriving the properties of the solution mapping since they will be important for determining ISS stability of the optimizer.

Lemma 2. *Under Assumptions 1–3, and with $\mathcal{A}$ defined in (11), the following hold:*

1) $\mathcal{A}$ is strongly monotone: $\langle u - v, y - z\rangle \geq \|y - z\|^2_{\bar{H}}$

2) $\mathcal{A}^{-1}$ is a co-coercive function:
$\langle \mathcal{A}^{-1}u - \mathcal{A}^{-1}v, u - v\rangle \geq \|\mathcal{A}^{-1}u - \mathcal{A}^{-1}v\|^2_{\widehat{H}}$

3) $\mathcal{A}^{-1}$ is Lipschitz continuous:
$\|\mathcal{A}^{-1}u - \mathcal{A}^{-1}v\|_{\widehat{H}} \leq \|u - v\|_{\widehat{H}^{-1}}$

for all $y, z \in \mathcal{Z}$ and $u \in \mathcal{A}(y), v \in \mathcal{A}(z)$.

Proof: 1) By monotonicity of the normal cone $\mathcal{N}_\mathcal{Z}$ [12], and $\mathcal{A} - \bar{H} = \mathcal{N}_\mathcal{Z}$

$$\langle u - \bar{H}y - v + \bar{H}z, y - z\rangle \geq 0,$$
$$\implies \langle u - v, y - z\rangle \geq \langle \bar{H}(y - z), y - z\rangle = \|y - z\|^2_{\widehat{H}},$$

.

2) Follows directly from 1 [15, Example 22.6].

3)Rewriting 2 yields

$$\begin{aligned}\|\mathcal{A}^{-1}u - \mathcal{A}^{-1}v\|^2_{\widehat{H}} &\leq \langle \mathcal{A}^{-1}u - \mathcal{A}^{-1}v, u - v\rangle \\ &\leq \left\langle \widehat{H}^{\frac{1}{2}}(\mathcal{A}^{-1}u - \mathcal{A}^{-1}v), \widehat{H}^{-\frac{1}{2}}(u - v)\right\rangle \\ &\leq \|\mathcal{A}^{-1}u - \mathcal{A}^{-1}v\|_{\widehat{H}}\|u - v\|_{\widehat{H}^{-1}},\end{aligned}$$

where the last line follows from the Cauchy-Schwartz inequality. Dividing by $\|\mathcal{A}^{-1}u - \mathcal{A}^{-1}v\|_{\widehat{H}}$ completes the proof.

Corollary 1. *Let Assumptions 1–3 hold, then for all $x, y \in \mathbb{R}^n$ the solution mapping is Lipschitz continuous i.e.*

$$\|S(x) - S(y)\|_{\widehat{H}} \leq \|\bar{G}(x - y)\|_{\widehat{H}^{-1}}. \tag{17}$$

B. ISS Gain of the Regularized Primal-Dual Method

Using the properties of the solution mapping, we can now show that the optimizer dynamics are ISS for the regularized primal-dual algorithm.

Theorem 2. *Consider the optimizer dynamics $z^+ = \mathcal{T}^\ell(z, x)$. Under Assumptions 1–3 , the error signal $e = z - S(x)$ is ISS with respect to the state update $\Delta x = x^+ - x$ and satisfies the bound*

$$\limsup_{k\to\infty} \|e_k\|_2 \leq \gamma_2(\ell, \epsilon) \limsup_{k\to\infty} \|\Delta x_k\|_{\widehat{H}^{-1}}, \tag{18}$$

where $\gamma_2 = b\rho^\ell/(1-\rho^\ell)$, $b = \|\hat{H}^{-\frac{1}{2}}\bar{G}\|_2$, and γ_2 is a class $\mathcal{L}$ function. The values of $\bar{G}$ and ρ are defined below (11) and in Theorem 1, respectively.

Proof: Using the results from Theorem 1 and Corollary 1 along with the triangle inequality, we have

$$\begin{aligned}\|z^+ - S(x^+)\|_2 &\leq \rho^\ell\|z - S(x^+)\|_2 \\ &= \rho^\ell\|[z - S(x)] + [S(x) - S(x^+)]\|_2 \\ &\leq \rho^\ell\|z - S(x)\|_2 + \rho^\ell\|\widehat{H}^{-\frac{1}{2}}[S(x^+) - S(x)]\|_{\widehat{H}} \\ &\leq \rho^\ell\|z - S(x)\|_2 + \rho^\ell b\|x^+ - x\|_{\widehat{H}^{-1}}\end{aligned}$$

where b contains the Lipschitz constant for S and $\widehat{H}^{-\frac{1}{2}}$ and $\rho \in (0, 1)$. If we let $e_{k+1} = z^+ - S(x^+)$ and $\Delta x_k = x^+ - x$ we arrive at

$$\|e_{k+1}\|_2 \leq \rho^\ell\|e_k\| + \rho^\ell b\|\Delta x_k\|_{\widehat{H}^{-1}}$$
$$\implies \|e_k\|_2 \leq \rho^{\ell k}\|e_0\| + \frac{\rho^\ell b}{1-\rho^\ell}\sup_{k\geq 0}\|\Delta x_k\|_{\widehat{H}^{-1}},$$

which concludes the proof.

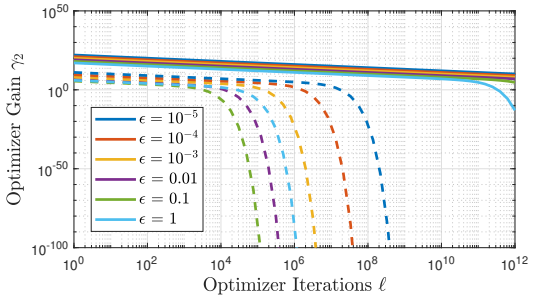

Fig. 3. Optimizer ISS gain computed from (18) for nominal MPC (solid lines) compared to CLP-MPC (dashed lines).

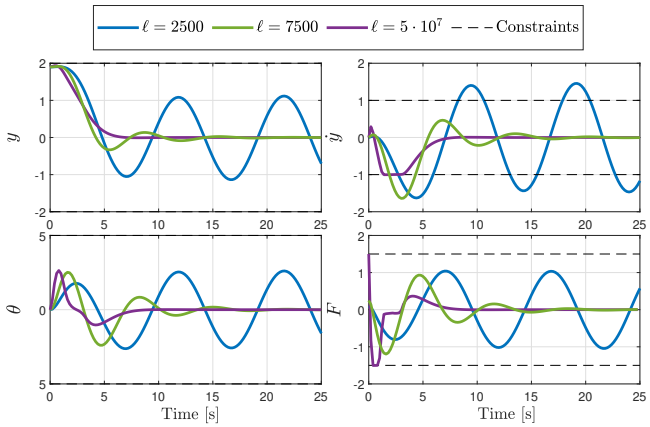

Fig. 4. Demostration of how increasing the number of iterations recovers stability and enforces constraints.

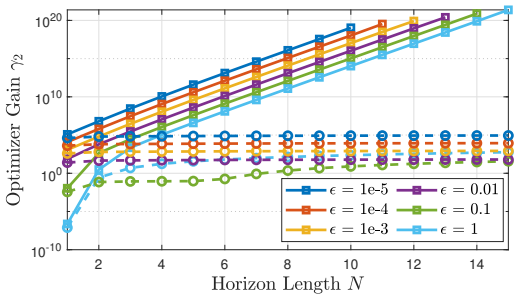

Fig. 5. Optimizer ISS gain compared to the horizon length under the nominal number of iterations. The solid lines represent nominal MPC, and dashed line represents CLP-MPC.

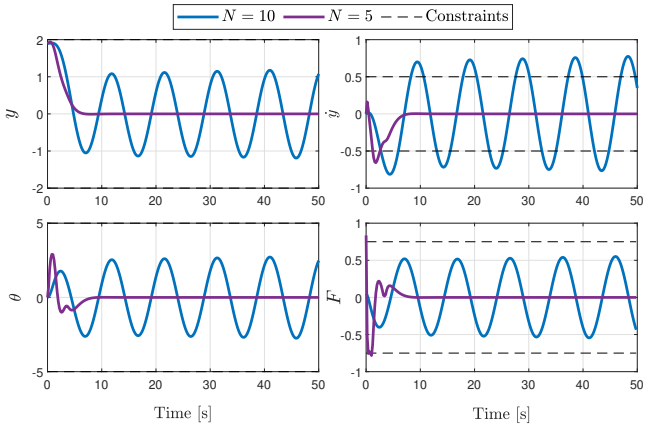

Fig. 6. Demonstration on how decreasing the horizon length recovers stability of the coupled system using the nominal $\boldsymbol{\ell = 2500}$.

C. Stability of the Coupled Optimizer-MPC System

The following well-known result proves ISS for nominal MPC with a varying additive disturbance e_k.

Theorem 3. *[16]: The ideal MPC law* (3) *is ISS with respect to the suboptimality error $e_k = z_k - S(x_k)$ and satisfies*

$$\limsup_{k\to\infty} \|x_k\| \leq \gamma_1 \limsup_{k\to\infty} \|\bar{B}e_k\|,$$

where $\bar{B} = B\Xi$ and γ_1 is a finite scalar.

Corollary 2. *Following from Theorems 2 and 3, the closed-loop system (4) is asymptotically stable if $\zeta\gamma_1\gamma_2(\ell, \epsilon) < 1$.*

Remark 3. *Corollary 2 is a direct application of the small-gain theorem [17]. Since $\gamma_2(\ell, \epsilon)$ is a monotonically decreasing function and $\zeta, \gamma_1 > 0$, $\exists \ell^*$ such that $\zeta\gamma_1\gamma_2(\ell, \epsilon) < 1$. Thus, the system can always be made asymptotically stable by performing a sufficient number of iterations.*

V. Numerical Examples

In the following sections, we will explore how the various optimizer parameters affect the ISS gain of the regularized primal-dual algorithm when coupled with both nominal and CLP-MPC. Consider the linearized inverted pendulum on a cart. The equations of motion are

$$4/3\ ml^2\ddot{\phi} - ml\ddot{y} = mgl\phi \tag{19a}$$
$$-ml\ddot{\phi} + (M+m)\ddot{y} = -b\dot{y} + F, \tag{19b}$$

where y is the position of the cart, ϕ is the angle of the pendulum, $g = 9.81\ \mathrm{m/s^2}$ is the gravitational constant, $M = 1\ \mathrm{kg}$ is the mass of the cart, and $m = 0.1\ \mathrm{kg}$, $b = 0.1\ \mathrm{Ns/m}$, and $l = 1\ \mathrm{m}$ are the mass, damping coefficient, and length of the pendulum respectively. The states and control inputs are $x = [y\ \ \dot{y}\ \ \phi\ \ \dot{\phi}]^T$ and $u = F$. The angle $\phi = 0$ corresponds to the upright position and the inverted pendulum dynamics are generated by linearization around the origin. Given the initial state $x_0 = [1.9\ 0\ 0\ 0]^T$, the control objective is to drive the system to the origin under constraints

$$\mathcal{X} = [-2,\ 2] \times [-0.5,\ 0.5] \times [-5^\circ,\ 5^\circ] \times [-5,\ 5],$$
$$\mathcal{U} = [-0.75,\ 0.75].$$

TDO-MPC is implemented using a sampling period of $t_s = 0.2\ s$, $Q = I$, $R = 1$, $N = 10$, $\epsilon = 10^{-4}$, $\ell = 2500$, and a solver tolerance of 10^{-8}. This choice of parameters is such that the interconnected MPC+optimizer is at the limit of instability. The following subsections detail how asymptotic stability can be recovered by choosing different parameters.

A. Influence of the number of Solver Iterations

As discussed in Remark 3, the most obvious way to attain closed-loop stability of TDO-MPC is by increasing the number of optimizer iterations per time step. Figure 3 shows how the optimizer gain γ_2 quickly tends to zero as long as a sufficient number of iterations are run. Additionally, it shows how the

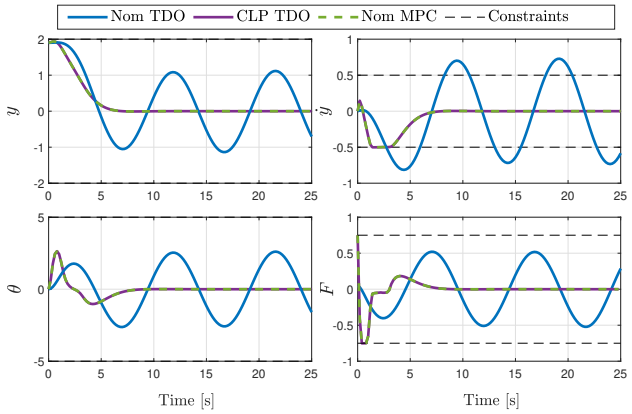

Fig. 7. Comparison between nominal MPC and CLP-MPC using the same number of iterations $\ell = \mathbf{2500}$. The CLP-MPC enforces constraints within $\mathbf{1\%}$ while the nominal MPC is unstable and requires at least $\ell = \mathbf{5 \cdot 10^7}$ iterations to enforce constraints.

conditioning number improvement seen in Figure 2 propagates to the optimizer gain γ_2.

Figure 4 shows how increasing the number of allowable iterations improves stability. An increase to $\ell = 7500$ iterations is sufficient to staiblize the system, but in order to enforce constraints to within a 1% threshold, the system requires at least $\ell = 5 \cdot 10^7$ iterations.

Although increasing the number of solver iterations is guaranteed to ensure stability, this solution goes against the general TDO philosophy of *reducing* computational complexity. The following sections investigate alternative strategies for stabilizing the interconnected MPC/optimizer system by improving the conditioning number of the OCP.

B. Influence of the prediction horizon length

For unstable systems, we see that the optimizer gain grows with the chosen horizon length since the dense QP formulation contains A^k terms. Figure 5 confirms this intuition and we see in Figure 6 that by decreasing the horizon length N, we are able to recover stability of our coupled system. Although reducing N may limit the feasibility region of (3), recent results [18] show that this can be offset throuh proper management of the reference.

C. Influence of the Closed-Loop Paradigm

Implementing the Closed-Loop Paradigm on TDO-MPC has shown significant improvements in decreasing the optimizer gain as seen in Figures 3 and 5. This is a direct consequence of using the LQR gain which removes the linear term from the QP and sets the Hessian's condition number to cond$(R + B^T P B)$. Moreover, when constraints are not being violated, the solution to the QP (16) becomes $\omega^* = 0$ and the coupled system is trivially stabilized by the internal LQR controller. This allows the online optimization algorithm to "focus" on enforcing constraints, significantly reducing the required number of iterations as illustrated in Figure 7.

VI. Conclusion

This paper analyzed a special case of TDO-MPC where we used a regularized primal-dual solver to enforce both input and state constraints for linear MPC. The solver sufficiently enforces constraints to within an arbitrary 1% threshold as long as the solver parameters are tuned properly. Additionally, we have shown that the Closed-Loop Paradigm achieves significant performance improvements in terms of minimum number of iterations required for constraint satisfaction. Future work includes decoupling the step size between the primal and dual variables and further exploring the benefits of the Closed-Loop Paradigm in TDO implementations.

References

[1] J. Rawlings and D. Q. Mayne, *Model Predictive Control: Theory and Design*. Madison, WI: Nob Hill Publishing, 2009.

[2] M. M. Nicotra, D. Liao-McPherson, and I. V. Kolmanovsky, "Time-distributed optimization for real-time model predictive control: Stability, robustness, and constraint satisfaction," *Automatica*, vol. 117, p. 108973, 2020.

[3] K. Yoshida, M. Inoue, and T. Hatanaka, "Instant MPC for linear systems and dissipativity-based stability analysis," *IEEE Control Systems Letters*, vol. 3, no. 4, pp. 811–816, 2019.

[4] M. M. Nicotra, D. Liao-McPherson, and I. V. Kolmanovsky, "Embedding constrained model predictive control in a continuous-time dynamic feedback," *IEEE Transactions on Automatic Control*, vol. 64, no. 5, pp. 1932–1946, 2019.

[5] M. Colombino, E. Dall'Anese, and A. Bernstein, "Online optimization as a feedback controller: Stability and tracking," *IEEE Transactions on Control of Network Systems*, vol. 7, no. 1, pp. 422–432, 2019.

[6] L. Grüne and J. Pannek, "Analysis of unconstrained NMPC schemes with incomplete optimization," *IFAC Proceedings Volumes*, vol. 43, no. 14, pp. 238 – 243, 2010.

[7] M. Diehl, R. Findeisen, F. Allgower, H. G. Bock, and J. P. Schloder, "Nominal stability of real-time iteration scheme for nonlinear model predictive control," *IEE Proceedings - Control Theory and Applications*, vol. 152, pp. 296–308, May 2005.

[8] S. Richter, C. N. Jones, and M. Morari, "Computational complexity certification for real-time MPC with input constraints based on the fast gradient method," *IEEE Transactions on Automatic Control*, vol. 57, no. 6, pp. 1391–1403, 2011.

[9] D. Liao-McPherson, T. Skibik, J. Leung, I. Kolmanovsky, and M. M. Nicotra, "An analysis of closed-loop stability for linear model predictive control based on time-distributed optimization," *IEEE Transactions on Automatic Control*, vol. 67, no. 5, pp. 2618–2625, 2022.

[10] J. Rossiter, *Model-Based Predictive Control*. Boca Raton, FL: CRC Press, 2017.

[11] R. T. Rockafellar, "Augmented lagrangians and applications of the proximal point algorithm in convex programming," *Mathematics of Operations Research*, vol. 1, no. 2, pp. 97–116, 1976.

[12] A. L. Dontchev and R. T. Rockafellar, *Implicit Functions and Solution Mappings*. Springer New York, 2014.

[13] J. Koshal, A. Nedić, and U. V. Shanbhag, "Multiuser optimization: Distributed algorithms and error analysis," *SIAM Journal on Optimization*, vol. 21, no. 3, pp. 1046–1081, 2011.

[14] A. B. Taylor, J. M. Hendrickx, and F. Glineur, "Exact worst-case convergence rates of the proximal gradient method for composite convex minimization," *Journal of Optimization Theory and Applications*, vol. 178, no. 2, pp. 455–476, 2018.

[15] H. H. Bauschke, P. L. Combettes, *et al.*, *Convex analysis and monotone operator theory in Hilbert spaces*, vol. 408. Springer, 2011.

[16] D. Limon, T. Alamo, D. M. Raimondo, D. M. de la Peña, J. M. Bravo, A. Ferramosca, and E. F. Camacho, *Input-to-State Stability: A Unifying Framework for Robust Model Predictive Control*, pp. 1–26. Berlin, Heidelberg: Springer Berlin Heidelberg, 2009.

[17] Z.-P. Jiang, Y. Lin, and Y. Wang, "Nonlinear small-gain theorems for discrete-time feedback systems and applications," *Automatica*, vol. 40, no. 12, pp. 2129–2136, 2004.

[18] T. Skibik, D. Liao-Mc Pherson, T. Cunis, I. V. Kolmanovsky, and M. M. Nicotra, "A feasibility governor for enlarging the region of attraction of linear model predictive controllers," *IEEE Transactions on Automatic Control*, pp. 1–1, 2021.